

Journal of Materials Chemistry A

Accepted Manuscript



This is an *Accepted Manuscript*, which has been through the Royal Society of Chemistry peer review process and has been accepted for publication.

Accepted Manuscripts are published online shortly after acceptance, before technical editing, formatting and proof reading. Using this free service, authors can make their results available to the community, in citable form, before we publish the edited article. We will replace this *Accepted Manuscript* with the edited and formatted *Advance Article* as soon as it is available.

You can find more information about *Accepted Manuscripts* in the [Information for Authors](#).

Please note that technical editing may introduce minor changes to the text and/or graphics, which may alter content. The journal's standard [Terms & Conditions](#) and the [Ethical guidelines](#) still apply. In no event shall the Royal Society of Chemistry be held responsible for any errors or omissions in this *Accepted Manuscript* or any consequences arising from the use of any information it contains.

Article

Predicting Electrochemical Properties and Ionic Diffusion in $\text{Na}_{2+2x}\text{Mn}_{2-x}(\text{SO}_4)_3$: Crafting a Promising High Voltage Cathode Material**Rafael B. Araujo^{*1}, M. S. Islam^{*1,3}, S. Chakraborty^{*1}, R. Ahuja^{1,2}**

¹*Condensed Matter Theory Group, Department of Physics and Astronomy, Box 516, Uppsala University, S-75120 Uppsala, Sweden.*

²*Applied Materials Physics, Department of Materials and Engineering, Royal Institute of Technology (KTH), S-100 44 Stockholm, Sweden.*

³*National University of Bangladesh, Gazipur-1704, DSHE, Dhaka-1000, Bangladesh.*

*1. Corresponding Author-1: muhammed.islam@physics.uu.se

*2. Corresponding author-2: rafael.baros@physics.uu.se

*3. Corresponding Author-3: sudiphys@gmail.com

Phone: 0184715874;

Abstract:

Sodium ion batteries have emerged as a good alternative to lithium based systems due to its low cost of production. In this scenario, the search for higher voltage, sodium cathodes results in a new promising *alluaudite* structure $\text{Na}_{2+2x}\text{Mn}_{2-x}(\text{SO}_4)_3$. The structural, electronic and Na diffusion properties along with defects has been reported in this investigation within the framework of density functional theory–A band gap of 3.61 eV has been computed and the average deintercalation potential is determined as 4.11 V vs. Na/Na⁺. Low concentration of anti-site defects is predicted due to their high formation energy. The biggest issue for the ionic diffusion in the $\text{Na}_{2+2x}\text{Mn}_{2-x}(\text{SO}_4)_3$ crystal structure reveals to be the effect of Mn vacancies increasing the activation energy of Na⁺ ions hop along the [0 0 1] equilibrium positions. This effect leads to activation energy values of almost the same high for the ionic hop through the [0 1 0] direction characterizing a 2D like ionic diffusion mechanism in this system.

Keywords: Sodium-ion battery, *Alluaudite*, $\text{Na}_{2+2x}\text{Mn}_{2-x}(\text{SO}_4)_3$, Diffusion, DFT study.

Introduction:

Among the rechargeable battery families, Lithium ion batteries (LIBs) have shown a rapid technological progress as energy storage systems (ESSs), with various portable electronic appliances in our modern daily life [1–3]. But the high demand and inadequate supply of Li in nature paves the way of possible usage of sodium ion batteries (SIBs) as a great alternative mainly in systems where specific capacity is not an issue. Sodium ion batteries (SIBs) have come up as more suitable than LIBs not only because of the natural abundance, but also the effective financial productivity and lower cost of raw materials are the other advantages. Therefore, a lot of theoretical and experimental efforts have been put in for the last few years in the scientific community to develop new sodium-based devices with higher redox potential and good kinetics [4-22].

Poly-anionic materials has become quite promising as far the cathode of SIBs [4-22] are concerned, because of their substantial thermal stability that come from strong covalent bonding of the structure. This definitely enhances the safety characteristics for these batteries [15, 23-27]. Recently, Yamada group proposed an *alluaudite* structure based on Fe redox centers as a new cathode material presenting higher redox potential, 3.8 vs. Na/Na⁺ with an excellent rate kinetics [28, 29, 30]. In order to further increase the redox reaction potential, D. Dwibedi *et. al.* [31] reported an *alluaudite* Na_{2+2x}Mn_{2-x}(SO₄)₃, with x=0.22, as a novel material with 4.4 V voltage vs. Na/Na⁺ as predicted by density functional theory calculations.

Na_{2+2x}Mn_{2-x}(SO₄)₃ has an *alluaudite* structure belonging to the C2/c space group [31]. The framework is basically built by Mn₂O₁₀ unites corner sharing with SO₄ tetrahedral. This crystal structure presents cavities along the c direction favoring the insertion and deinsertion of Na ions. To the best of our knowledge, there is no studies unveiling the electrochemistry and kinetics of the battery using Na_{2+2x}Mn_{2-x}(SO₄)₃ as a cathode material.

Based on the density functional theory (DFT) calculations, the electronic properties, open circuit voltage and diffusion mechanisms to Na_{2+2x}Mn_{2-x}(SO₄)₃ have been studied with the essential idea of improving its applicability as a cathode material. A band gap of 3.61 eV is computed together with an open circuit voltage of 4.11 V for

half-sodiation reaction. These results are in reasonable agreement with the reported values [31]. The formation energy calculations of the intrinsic defects reveal an unlikely formation of anti-site defects in the [001] channels of the $\text{Na}_{2+2x}\text{Mn}_{2-x}(\text{SO}_4)_3$ crystal structure. On the other hand, the Mn vacancies showed to play a prime role in sodium ions diffusion mechanism. In fact, the Mn vacancies block the ionic diffusions through [0 0 1] channels of the *alluaudite* structure forcing the ions to move also through the [0 1 0] direction.

2. Computational details:

Electronic structure calculations have been performed within the density functional theory (DFT) framework based on the projector augmented wave method (PAW) as implanted in the Vienna *Ab-initio* Simulation Package (VASP) [32, 33]. All the calculations have been performed using the spin-polarized formalism in the Perdew, Burke, and Ernzerhof (PBE) parameterization for the exchange and correlation functional [34]. The self-interaction error has been taken care of by considering GGA+U implementation by Dudarev *et. al.* [35]. The Hubbard repulsion term U and the exchange term J are represented using a single parameter $U_{\text{eff}}=U-J$ and the value of U_{eff} has been taken from Ref. [36] amounting 3.9 eV. A super-cell of 1a x1b x3c repetition and 231 atoms has been considered throughout the calculation. This super-cell size avoids interaction between periodic images of the defects. These calculations are carried out with a single Γ k-mesh and an energy cut-off of 600 eV has been set for all expanded wave functions.

The formation energy of the defects are computed using the following equation [37]:

$$E_f(X^q) = E_0(X^q) - E_0(\text{bulk}) - \sum_i n_i \mu_i$$

where, $E(X^q)$ is the defect formation energy, $E_0(X^q)$ is the energy of the super-cell with the defect, $E_0(\text{bulk})$ is the total energy of the bulk system without the defect, μ_i and n_i are the chemical potential and the number of atom of species i removed from the super-cell. For sodium it was set by ion exchange with the anode [38]. To compute the activation energy barrier, the climbing-image nudged elastic band method (cNEB) has been employed [39, 40]. For each performed cNEB calculation up to five images is linearly interpolated between the two equilibrium sites.

In order to obtain the most stable position of the sodium atoms and a profound insight of the ionic diffusion mechanisms in $\text{Na}_{2+2x}\text{Mn}_{2-x}(\text{SO}_4)_3$, an ab initio molecular dynamics (AIMD) has been performed. Velocities were allowed to scale each 4 steps at $T = 600$ K to set the kinetic energy of the system to a specific value. In the intermediated period, a micro-canonical ensemble is simulated. This temperature was selected with the aim of accelerated the dynamics. The simulation was performed in 48 ps. With the results of the AIMD simulation new energy minimizations were carried out. At this step fractional atomic coordinates coming from the AIMD in each 3000 steps were considered amounting 16 new optimization processes. From these 16 new calculations, the optimized structure, which shows the lower energy, was chosen as the most stable and a representative fractional set of atomic positions for the referent poly-anion is derived.

3. Results and Discussions:

3. a. Crystal and Electronic Structural Analysis

The recently synthesized $\text{Na}_{2+2x}\text{Mn}_{2-x}(\text{SO}_4)_3$ has an *alluaudite* structure belonging to the $C2/c$ space group as depicted in Fig. 1. In this framework octahedral Mn sites, MnO_6 , share oxygen atoms forming bi-octahedral units, Mn_2O_{10} . These units are also repeatedly connected with tetrahedral SO_4 units forming tunnel in the $[001]$ direction, through which Na^+ ions can migrate. It has been already [31] reported that sodium atoms have been distributed among three main sites, Na1, Na2 and Na3, where each of them presents 1, 0.64 and 0.80 partial occupancies. Moreover, Mn atoms assume fractional occupancy of 0.89.

In order to construct a correct model system, a super-cell with $1 \times 1 \times 3c$ repetition containing 231 atoms and 12 formula units of $\text{Na}_{2+2x}\text{Mn}_{2-x}(\text{SO}_4)_3$ with $x=0.25$ ($\text{Na}_{2.5}\text{Mn}_{1.75}(\text{SO}_4)_3$) has been considered. Mn vacancies are created by choosing three different configurations of the crystal structure and then a energetic minimization of the fractional coordinates have been performed. The configuration with the minimum ground state energy was set as the more suitable to represent this material.

To describe the right fractional coordination of Na atoms a different methodology has been employed. Initially, all positions with fractional occupancy equal 1, Na1, are occupied by a sodium ion. Then, the remaining sodium atoms are

distributed proportionally with the fractional occupancies presented by them. The excess sodium atoms are distributed between the Na2 and Na3 atomic positions. After getting the optimized structure, a molecular dynamics process has been performed at $T=600$ K. This temperature helps to accelerate the dynamics of the reaction. Then, for each 3000 steps of the molecular dynamics a single optimization procedure of the coordinates is allowed and 16 new structures have emerged from this methodology. Once more, the structure presenting lower energy has been selected as the ground state. The investigation of the lowest energy structure has presented a new Na position. In fact, each Mn vacancy has been occupied by an excess Na forming a new site for these atoms named here as NaMn.

With the primer objective of computing the volumetric change and to derive the redox potential energy, the half-sodiated structure has also been investigated. In this case, sodium atoms in the Na1 position were maintained in the crystal structure of the host material. Figure 01 depicts the optimized structure for $\text{Na}_{2+2x}\text{Mn}_{2-x}(\text{SO}_4)_3$ and Tab. 1 shows the average magnetic moment per Mn atom, lattice constants and super-cell volume for the sodiated ($\text{Na}_{2.5}\text{Mn}_{1.75}(\text{SO}_4)_3$) and half-sodiated ($\text{Na}_{1.25}\text{Mn}_{1.75}(\text{SO}_4)_3$) crystal structures.

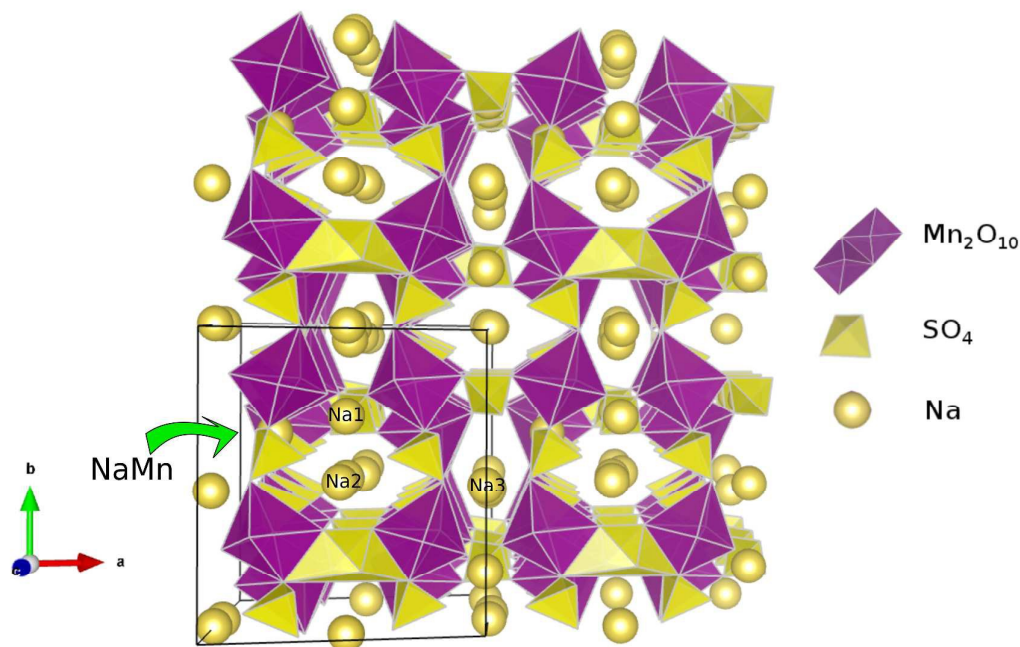


Figure 01: Schematic crystal structure representation of $\text{Na}_{2.5}\text{Mn}_{1.75}(\text{SO}_4)_3$. SO_4 tetrahedral is represented in yellow. Mn_2O_{10} bi-octahedral is represented in pink.

Na_1 , Na_2 , Na_3 are the 3 distinct Na sites in the alluaudite structure. $NaMn$ is the site created with the removal of Mn. VESTA [41]

Table1: Magnetic moment μ_B , optimized lattice parameters and volume of the unit cell. The experimental values were taken from Ref. [34]

Systems	μ (μ_B)	a (Å)	b (Å)	c (Å)	A(°)	B(°)	Γ (°)	Vol. (Å ³)
Na_{2.5}Mn_{1.75}(SO₄)₃	4.66	12.66	12.63	6.64	90.34	116.25	90.60	965.32
Exp		12.80	12.95	6.68	90.00	115.76	90.00	983.32
Na_{1.25}Mn_{1.75}(SO₄)₃	4.38	12.53	12.54	19.36	89.91	114.61	89.92	922.66

The analysis of Tab. 01 reveals an agreement between the computed lattice parameters and the corresponding experimental values with discrepancy smaller than 2%. This result is in the general trend under the GGA framework with small discrepancies of the lattice parameters with respect to the experimental values. The spin-polarized GGA + U calculations with ferromagnetic configuration can give reasonable prediction about the structural parameters for the full-sodiated compound. It is worth to mention that sodium deintercalation reaction has been occurred with a small volumetric change of 1.8 %.

The average bond lengths between the transition metal and sulfur ions with the oxygen ions in the full-sodiated and half-sodiated states for $Na_{2-2x}Mn_{2x}(SO_4)_3$ have been computed as well. The average bond length of MnO_6 octahedral is directly associated with the oxidation state of the transition metal [42]. In fact, when the oxidation occurs in TM centers one electron from an anti-bond orbital of Mn-O bonds is removed resulting in MnO_6 bond length shrinkage. The average bond length of MnO_6 in $Na_{2.5}Mn_{1.75}(SO_4)_3$ is 2.20 Å while in the half-sodiated structure, the value becomes 2.14 Å. For S-O bonding 1.49 Å is computed value. Indeed, the strong covalent bonds between S-O do not get affected by the oxidation and reduction reaction of the battery. This is one of the responsible factors behind the reasonable structural stability in the framework.

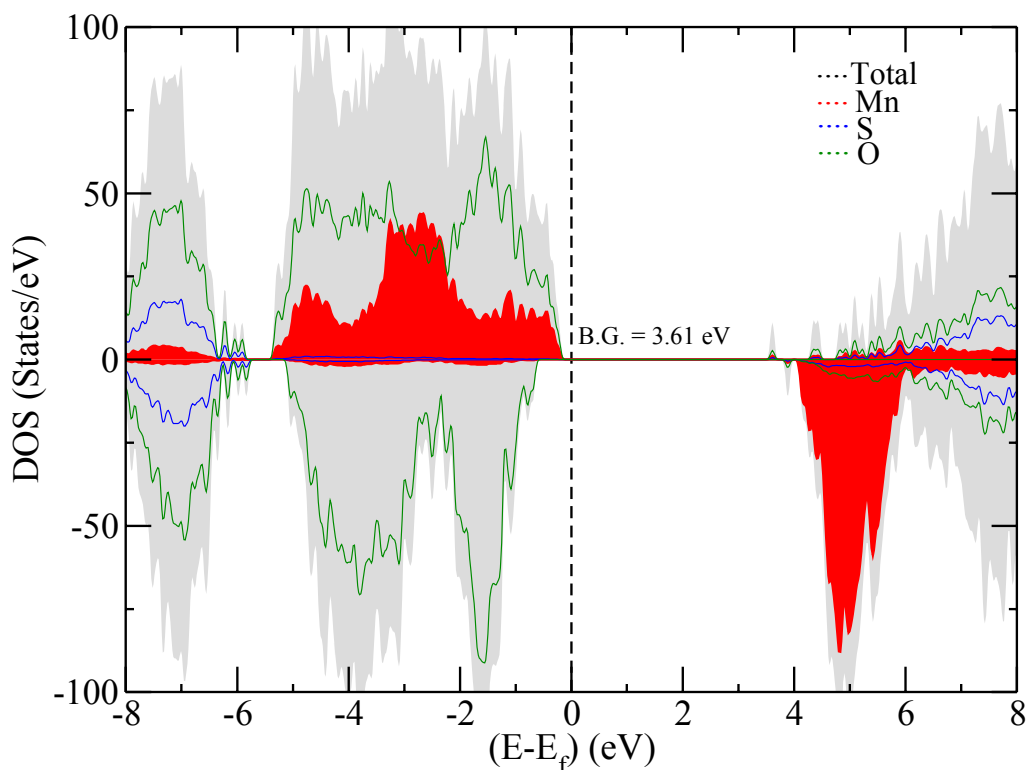


Figure 02: Total density of states (DOS) and the projected density of states (pDOS) of $\text{Na}_{2-2x}\text{Mn}_{2x}(\text{SO}_4)_3$ drawn by using the GGA+U scheme. The black color curve line displays the total DOS, while the red, blue and green colors curve lines show the summed up contributions of the pDOS for manganese, sulfur and oxygen atoms, respectively.

The total density of states (DOS) and the partial density of states (pDOS) of $\text{Na}_{2.5}\text{Mn}_{1.75}(\text{SO}_4)_3$ system, calculated using GGA+U scheme, are showed in Fig. 02. The main results captured by the pDOS follow the general characteristic of the current poly-anion used as cathode material [43-45]. The band gap value is 3.61 eV with a semiconductor like behavior. The main contribution to the valence band maxima originates from Mn and O atoms. This result leads to the fact that the oxidation process is occurring in the oxygen and Mn sublattices of $\text{Na}_{2.5}\text{Mn}_{1.75}(\text{SO}_4)_3$. This fact has also been supported by the computed magnetization per Mn atom. The value of magnetization per Mn atom is varying from $4.29 \mu_B$ up to $4.50 \mu_B$ with an average value of $4.38 \mu_B$ in the half-sodiated material while for the full-sodiated structure it

shows $4.66 \pm 0.01 \mu_B$ per Mn atom. It means that the oxidation reaction induced by the removal of Na atoms from the crystal structure of $\text{Na}_{2.5}\text{Mn}_{1.75}(\text{SO}_4)_3$ is not experimented only for the Mn atoms close to the created sodium vacancy. In fact, all Mn sub-lattices are somehow participating. Moreover, oxygen atoms also present some small magnetic moment in the half-sodiated material, which, together with the high contribution of O atoms at the Fermi level, confirms the hypothesis that the oxygen anionic sub-lattice together with the Mn sub-lattice participates in the oxidation and reduction reaction of the battery.

The average deintercalation voltage vs. Na/Na^+ has been computed as described in Ref. [46]. The calculated voltage presents 4.11 V vs. Na/Na^+ . This results is in good accordance with the reported 4.4 V by D. Dwivedi *et al.* [31]. The calculation of the voltage, in this case, has been done considering an half-sodiated crystal structure of the type $\text{Na}_{1.25}\text{Mn}_{1.75}(\text{SO}_4)_3$, where all sodium atoms located in Na1 sites are maintained in its crystal structure.

3. b Defect Formation Energy

During the cell reaction many point defects could be created in the crystal structure of the cathode material. To have a better understanding of the electrochemical behavior of the device it is essential to investigate the defect properties of the electrode crystal structure. For example, the investigation of defects where Na^+ exchanges position with the transition metal center (anti-site defects) is of significant interest for cathode compounds. In systems where the ionic diffusion process occurs in 1 dimension such as LiFePO_4 this kind of defect can hinder the ionic diffusion process compromising the device performance. [47].

The formation energy for sodium vacancies and for anti-site defects, where Na^+ exchanges position with one Mn^{+2} is computed for $\text{Na}_{2.5}\text{Mn}_{1.75}(\text{SO}_4)_3$. In order to evaluate these quantities, a pair of Na^+ and an electron are removed from this poly-anion by creating a neutral vacancy V_0^{Na} . For the anti-site defect, three distinct possibilities have been taken into account. In the first case, Mn^{+2} ion undergoes an exchange of position with sodium occupying a Na1 position. Mn^{+2} are exchanged with Na2 and Na3 sodium ions in the second and third cases, respectively. The results of the formation energy of the defect sites are summarized in Table 02 with the lower formation energy for each Na site.

Table 02: Formation energy in eV of V_0^{Na} vacancies and anti-site defects Na/Mn.

Sodium defects	Formation energy (eV)
Na3	0.71
Na2	0.89
Na1	0.95
Na-Mn	1.39

Anti-site defects	Formation energy (eV)
Na3/Mn	2.04
Na2/Mn	2.48
Na1/Mn	1.83

From the formation energy values depicted in Tab. 02, it is seen that the anti-site defects of type Na/Mn are unfavorable in $\text{Na}_{2.5}\text{Mn}_{1.75}(\text{SO}_4)_3$ due to the high formation energy. This result is in contrast with very well established materials such as LiMPO_4 (M=Fe, Mn and Co) [47, 48], where the exchange of transition metals with Li^+ is a problem. Clark et. al. [49] has also found similar results in comparison with the reported results for the compound $\text{Li}_2\text{M}(\text{SO}_4)_2$ (M=Fe, Mn and Co) where anti-site defects were shown to be unfavorable.

The analysis of the structural changes with the creation of the Na3/Mn anti-site defect shows that the substitution of Na^+ in the Mn^{+2} position moves away the surrounded oxygen atoms. Initially, the average bond distance of the Mn-O octahedral 2.19 Å. Exchanging the Na atom with Mn, the newly formed bonds between Na-O produce an average distance of 2.22 Å. Moreover, the closest Na atoms move even closer from Na defective position. This local change in the $\text{Na}_{2.5}\text{Mn}_{1.75}(\text{SO}_4)_3$ environment results in a lack of negative charge in this region of the structure. Indeed, Mn centers are able to donate two electrons to the compound forming Mn^{+2} while the sodium atoms only comes with one electron forming Na^+ . Then, there exists a lack of local negative charge forcing the system to rearrange itself. Moreover, the atomic radius of the Na ions is bigger than the revealed value of manganese. It also induces a local structural change. Therefore, the local structural changes resulting from the anti-site defect formation appears as a result of these two effects.

From Tab. 02, one can observe that Na3 position is the most probable one for the creation of a vacancy V_0^{Na} due to its lower formation energy. Moreover, the NaMn presents the greater formation energy value.

In disagreement with systems like LiFePO_4 where the formation of Li vacancies emerge with a polaron formation in the closest Fe site [47], the formation of V_0^{Na} vacancy in $\text{Na}_{2.5}\text{Mn}_{1.75}(\text{SO}_4)_3$ does not follow this trend. Figure 01 of the supplementary material is presenting the charge-density difference ($\Delta \rho(\mathbf{r})=$

$\rho(\text{Na}_{2.5}\text{Mn}_{1.75}(\text{SO}_4)_3) - \rho(\text{Na}_{2.5}\text{Mn}_{1.75}(\text{SO}_4)_3\text{-defective}) + \rho(\text{Na})$) where ρ is the charge-density of a Na placed in one of the site positions. Therefore, one can see that the charge movement occurs by donating electrons for some oxygen ions as well as to some Mn atoms. This analysis is highly supported by pDOS showed in Fig. 02 where the oxygen states together with Mn states appear with larger contribution in valence band minimum.

3. c. Diffusion mechanism of Na ions.

The investigation of Na ion diffusion mechanisms in $\text{Na}_{2.5}\text{Mn}_{1.75}(\text{SO}_4)_3$ is of real importance as far the battery performance concerned. In fact, the transport properties assumed by Na ions in the cathode compound largely influence the rate of the battery reaction. The energy barrier of such Na diffusion process in the crystal structure of $\text{Na}_{2.5}\text{Mn}_{1.75}(\text{SO}_4)_3$ has been investigated based DFT approach.

Four main possible pathways for the ionic transport have been considered in this investigation. The choice of these ionic diffusion pathways is driven by the AIMD simulation insights and the reported diffusion mechanisms in Re. [50]. Figure 02 of the supplementary material displays the snapshots of the *ab initio* molecular dynamics.

In the first case, Na^+ hopping through the [001] direction with the V_0^{Na} vacancy moving from Na2 to Na2 positions has been investigated. The second path is also in [001] direction, while the vacancy moves through the Na3 main positions. The third pathway hops from a Na3 to Na1 and then to Na2 position. The fourth pathway accounts for the migration of V_0^{Na} by leaving Na2 to NaMn and then going to Na3 position. Figure 03 is representing these possibilities and in Tab. 03 the highest and lowest activation energies for each case are summarized.

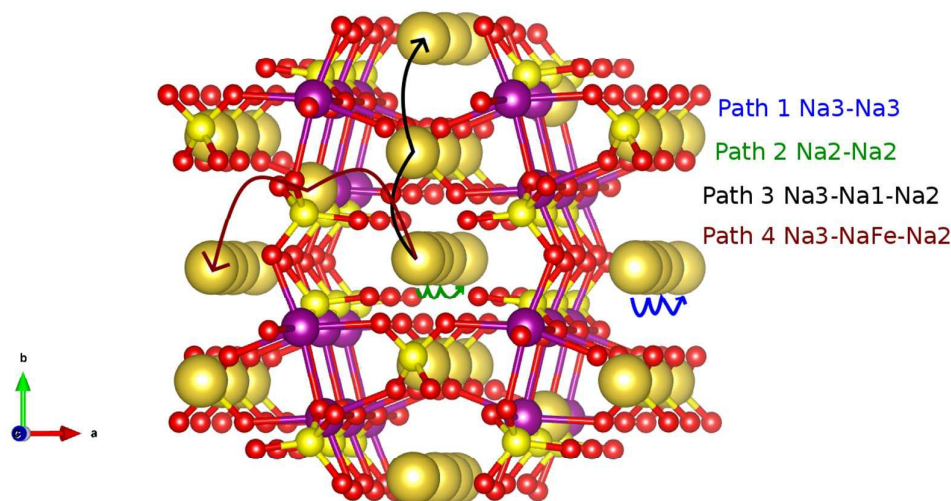


Figure 03 : Illustrative picture of the investigated Na^+ diffusion pathways in the crystal structure of $\text{Na}_{2.5}\text{Mn}_{1.75}(\text{SO}_4)_3$.

Table 03: Highest and lowest migration activation energies for each investigated pathway.

Pathway	Highest activation energy (eV)	Lowest activation energy
Na3-Na3	0.74	0.31
Na2-Na2	0.96	0.46
Na3-Na1-Na2	0.58	0.57
Na2-NaMn-Na3	1.29	1.20

The results from the cNEB have shown the pathway 1 as the most likely pathway with an activation energy varying from 0.31 eV to 0.74 eV. The hopping distance between local minima are about 5 Å in this pathway Fig. 04 (a) shows the different activation energies for Na^+ migration in this path.

As reported by Wong *et. al.* [50] the distance of the accounted hop from the transition metal vacancy is a possible concern. This fact can explain why higher activation energies are computed between the reactions coordinates 8 Å and 10 Å in Fig. 04 (a). As it is mentioned before, Mn atoms donate two electrons to the crystal framework. The removal of a Mn atom is accompanied of a charge absence in the close surround of the structure. Then, it is speculated that the greater activation energies displayed in some hops, for example in the hop between 8 Å and 10 Å of pathway 01, comes due to this local charge arrangement. The snapshots of the AIMD are plotted in Fig. 2 of the supplementary material. It is clear, from there, that sodium ions have spent a longer time in some specific positions of the pathway 1 due to the presented larger activation energy of some hops.

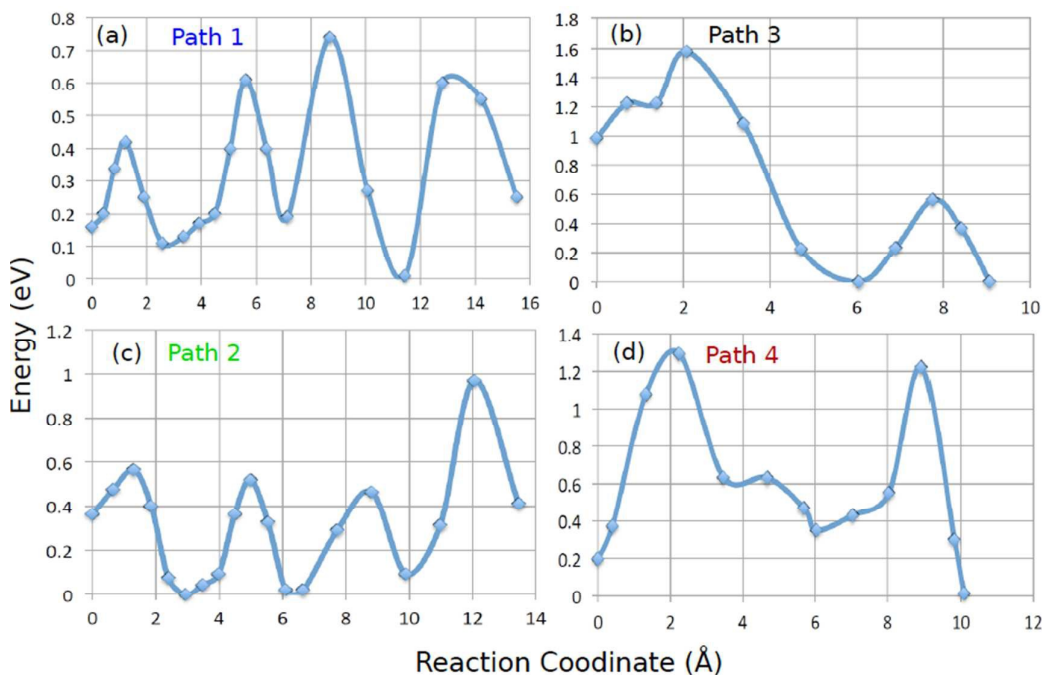


Figure 04: Activation energy derived from the *cNEB* method in the considered pathways for $\text{Na}_{2.5}\text{Mn}_{1.75}(\text{SO}_4)_3$.

Figure 04 (c) shows the activation energy for the migration of V_0^{Na} in pathway 2. The greater activation energy value computed for this path is 0.96 eV, which is 0.22 eV higher than the activation energy for pathway 1 and the smaller value is 0.46 eV that is still higher than the revealed value for the lower activation energy in pathway 1. This result confirms the hypothesis that the diffusion mechanism in $\text{Na}_{2.5}\text{Mn}_{1.75}(\text{SO}_4)_3$ is most dominated by pathway 1. Disordered Mn vacancies appear to induce greater barrier also in this direction leading to 0.96 eV activation energy. This higher activation energy value for the hop between 12 Å and 16 Å in pathway 2, confirms the dependence of Na^+ migration mechanism on Mn defects.

The activation energies corresponding to the pathway 3 reveal energy barriers of 0.58 eV and 0.57 eV for the two considered hopping. Initially, the vacancy moves from Na3 to Na1 position. This migration displays 0.58 eV barrier as shows in Fig. 04 (b). Indeed, it is very likely that the ions come diffusing through the pathway 1. As discussed before, the greater activation energy due to the Mn vacancies block the Na^+ migration with barriers of about 0.74 eV. At this point, it is easier to change direction and migrates in the 0.56 eV barriers displayed in path 3. This result is also supported

properly by the molecular dynamic snap shots, which has been shown in Fig. 02 of the supplementary material. There the diffusion of Na^+ atoms through path 3 is quite clear. Path 4 has been emerged with activation energies of about 1.29 and also 1.20 eV. These high values make the migration mechanism unlikely for this pathway.

A general agreement has been observed while comparing the obtained results for the ionic diffusion mechanism in $\text{Na}_{2.5}\text{Mn}_{1.75}(\text{SO}_4)_3$ and the reported results by L. L. Wong, [50] where it was reported that the hopping between equilibrium points through Na3-Na3 as the dominant diffusion path with an activation barrier of 0.28 eV as one of the possible pathways of the structural model. While observing the first saddle point in Fig. 04 (a), activation energy of 0.31 eV is found that is close to the reported result in Ref. [50]. For the sodium ion diffusion in pathway 2 (Na2-Na2), the smaller activation energy has been found as 0.46 eV. This result also follows the reported trend where the activation energy of the Na3-Na3 hops present as the most likely. The main differences concerning to the reported results of this work and the reported in [50] come from two primary sources. The first one is the used structural model. Here, higher concentration of transition state metal vacancies are included and, as a consequence, the blocking of the Na^+ diffusion for the [001] direction comes with a distinct shape. The second and more obvious is the usage of Mn instead of Fe as the redox center in the *alluaudite* structure.

The sodium diffusion coefficient (D_{Na}) has been derived from the mean square displacement shown in Fig. 03 of the supplementary material. The D_{Na} has been evaluated as $D_{\text{Na}} = (1/6t) \{[\mathbf{r}(t)]\}^2$ where \mathbf{r} is the position as a function of time t [51]. Only values after 10 ps were considered for the calculation of the diffusion coefficient since these 10 ps were reserved for equilibrate the system. The value of the diffusion coefficient (D_{Na}) is $6 \times 10^{-8} \text{ cm}^2/\text{s}$ that is in the range of present cathode materials [51, 52]. It is also possible to see from the slop of the MSD that almost no self-diffusion is observed for the other ions. This result indicates that Mn atoms would not exchange position with Na atoms as showed by the defect formation energies. It confirms the fact that anti site defects do not play a significant role in this system.

To gain the insight about the most dominant ionic migration mechanism at $T=600 \text{ K}$, the diffusion coefficient is related to the activation energies shown in Tab. 03 that has been computed using the standard Arrhenius relation as explained in Fig. 05 of the supplementary material. An extrapolation of the activation energy correlated to the diffusion coefficient computed using the MSD emerged with an

energetic average barrier of 0.53 eV. This indicates that the Na3-Na1-Na2 pathway dominates the sodium ion migration at this temperature. It is very likely that Na ions hop through the c channels (pathway 1 and 2) turn to the b direction when the higher activation energies are presented. With this picture, while the Na ion moves in the c channel it would be filling activations energy of about 0.31 eV. Then, the high activation energy blocks this path and the Na ion moves its direction to [0 1 0]. In this way the highest activation energy felt by the Na ion reaches 0.57 eV what is in really good agreement with the value extrapolated with the MD simulation.

CONCLUSIONS

Density functional theory has been employed to investigate the electrochemistry as well as the kinetic of $\text{Na}_{2+2x}\text{Mn}_{2-x}(\text{SO}_4)_3$ as a cathode material for sodium based batteries. The main conclusions of this investigation can be summarized as follows:

1. **Structural and electronic properties:** The structural model used to represent $\text{Na}_{2+2x}\text{Mn}_{2-x}(\text{SO}_4)_3$ reveals to be in reasonable good agreement with the experimental results. A tendency has been observed that part of the excess sodium moves to Mn vacancies position ensuring a better local charge balance. $\text{Na}_{2+2x}\text{Mn}_{2-x}(\text{SO}_4)_3$ reveals a band gap of 3.61 eV together with an average redox potential of 4.11 V vs. Na/Na^+ . The oxidation reaction occurs via Mn and O sub-lattices ensuring a quite small volume change in the (de)intercalation reaction.
2. **Defect formation:** The formation energy of the intrinsic defects such as antisite and sodium defects display low values leading to small defect concentration in $\text{Na}_{2+2x}\text{Mn}_{2-x}(\text{SO}_4)_3$ crystal structure.
3. **Ionic migration:** To understand the migration mechanism of sodium atoms in $\text{Na}_{2+2x}\text{Mn}_{2-x}(\text{SO}_4)_3$ structure, the activation energies of 4 possible diffusion paths are investigated extensively. It is shown that the hop between Na3 positions (Path 01) along [0 0 1] direction is the most likely with activation energies of about 0.31 eV. However, the Mn deficiency blocks the ionic diffusion-creating barrier as high as 0.76 eV for the one-dimensional migration. With this scenario, the ionic diffusion turns to an alternative mechanism hoping from Na3-Na1-Na2 (Path 03) with activation energy of 0.58 eV. This pathway points to [010] direction working as a link between the diffusion of Na2-Na2 and Na3-Na3 hops. Through the MSD, the diffusion coefficient at $T = 600$ K have been evaluated amounting 10^{-8} cm^2/s . It confirms the good kinetic

properties of $\text{Na}_{2+2x}\text{Mn}_{2-x}(\text{SO}_4)_3$. Moreover, 2D like ionic diffusion mechanism is predicted.

Acknowledgement:

The corresponding authors are thankful to Erasmus Mundus and Swedish Institute for a doctoral and Post Doctoral fellowship respectively. We would like to acknowledge the Carl Tryggers Stiftelse for Vetenskaplig Forskning (CTS), Swedish Institute (SI), Swedish Research Council (VR), Swedish Energy Agency and StandUP for financial support. SNIC, HPC2N and UPPMAX are acknowledged for providing computing time.

References

- [1] H. Li, Z. Wang, L. Chen and X. Huang, *Adv. Mater.*, 2009, 21, 4593–4607. □
- [2] J. B. Goodenough and Y. Kim, *Chem. Mater.*, 2010, 22, 587–603. □
- [3] J. B. Goodenough and K. S. Park, *J. Am. Chem. Soc.*, 2013, 135, 1167–1176. □
- [4] B. L. Ellis, W. R. Makahnouk, Y. Makimura, K. Toghill and L. F. Nazar, *Nat. Mater.*, 2007, 6, 749–753. □
- [5] F. Sauvage, L. Laffont, J. M. Tarascon and E. Baudrin, *Inorg. Chem.*, 2007, 46, 3289–3294. □
- [6] A. Abouimrane, D. Dambournet, K. W. Chapman, P. J. Chupas, W. Weng and K. Amine, *J. Am. Chem. Soc.*, 2012, 134, 4505–4508. □
- [7] M. D'Arienzo, R. Ruffo, R. Scotti, F. Morazzoni, C. M. Mari and S. Polizzi, *Phys. Chem. Chem. Phys.*, 2012, 14, 5945–5952.
- [8] J. Qian, M. Zhou, Y. Cao, X. Ai and H. Yang, *Adv. Energy. Mater.*, 2012, 2, 410–414.
- [9] S. Tepavcevic, H. Xiong, V. R. Stamenkovic, X. Zuo, M. Balasubramanian, V. B. Prakapenka, C. S. Johnson and T. Rajh, *Acs Nano*, 2012, 6, 530–538. □
- [10] N. Yabuuchi, M. Kajiyama, J. Iwatate, H. Nishikawa, S. Hitomi, R. Okuyama, R. Usui, Y. Yamada and S. Komaba, *Nat. Mater.*, 2012, 11, 512–517. □
- [11] Y. Lu, L. Wang, J. Cheng and J. B. Goodenough, *Chem. Commun.*, 2012, 48, 6544–6546.

- [12] P. Barpanda, J. Chotard, N. Recham, C. Delacourt, M. Ati, L. Dupont, M. Armand and J. Tarascon, *Inorg. Chem.*, 2010, 49, 7401–7413.
- [13] K. Trad, D. Carlier, L. Croguennec, A. Wattiaux, M. Ben Amara and C. Delmas, *Chem. Mater.*, 2010, 22, 5554–5562.□
- [14] K. Trad, D. Carlier, A. Wattiaux, M. B. Amara and C. Delmas, *J. Electrochem. Soc.*, 2010, 157, A947–A952.□
- [15] R. Tripathi, T. N. Ramesh, B. L. Ellis and L. F. Nazar, *Angew. Chem. Int. Ed.* 49, 2010, 8738–8742.□
- [16] J. Zhao, J. He, X. Ding, J. Zhou, S. Wu and R. Huang, *J. Power Sources*, 2010, 195, 6854–6859.□
- [17] K. T. Lee, T. N. Ramesh, F. Nan, G. Botton, and L. F. Nazar, *Chem. Mater.*, 2011, 23, 3593–3600.□
- [18] P. Barpanda, T. Ye, S. Nishimura, S. Chung, Y. Yamada, M. Okubo, H. Zhou and A. Yamada *Electrochem. Commun.*, 2012, 24, 116–119.□
- [19] H. Chen, G. Hautier and G. Ceder, *J. Am. Chem. Soc.*, 2012, 134, 19619–19627.□
- [20] A. Jain, G. Hautier, C. Moore, B. Kang, J. Lee, H. Chen, N. Twu and G. Ceder, *J. Electrochem. Soc.*, 2012, 159, A622.□
- [21] J. Kang, S. Baek, V. Mathew, J. Gim, J. Song, H. Park, E. Chae, A. K. Rai and J. Kim, *J. Mater. Chem.*, 2012, 22, 20857.□
- [22] H. Kim, I. Park, D. Seo, S. Lee, S. Kim, W. J. Kwon, Y. Park, C. S. Kim, S. Jeon and K. Kang, *J. Am. Chem. Soc.*, 2012, 134, 10369–10372.□
- [23] B. L. Ellis, W. R. M. Makahnouk, W. N. Rowan-Weetaluktuk, D. H. Ryan and L. F. Nazar, *Chem. Mater.*, 2010, 22, 1059–1070.
- [24] K. Trad, D. Carlier, L. Croguennec, A. Wattiaux, M. Ben Amara and C. Delmas, *Inorg. Chem.*, 2010, 49, 10378–10389.
- [25] Y. Liu, Y. Xu, X. Han, C. Pellegrinelli, Y. Zhu, H. Zhu, J. Wan, A. C. Chung, O. Vaaland, C. Wang and L. Hu, *Nano Lett.* 12, 2012, 5664–5668.
- [26] R. A. Shakoor, D. Seo, H. Kim, Y. Park, J. Kim, S. Kim, H. Gwon, S. Lee and K. Kang, *J. Mater. Chem.*, 2012, 22, 20535.
- [27] Z. Jian, L. Zhao, H. Pan, Y. S. Hu, H. Li, W. Chen and L. Chen, *Electrochem. Commun.*, 2012, 14, 86–89.□
- [28] P. Barpanda, G. Oyama, S. Nishimura, S. Chung and A. Yamada, *Nature Communications*, 2014, 5, 4358.
- [29] J. Ming, P. Barpanda, S. Nishimura, M. Okubo and A. Yamada *Electrochem Commun.*, 2015, 51, 19–22.
- [30] P. Barpanda, *Isr. J. Chem.*, 2015, 55, 537–557.

- [31] D. Dwibedi, R. B. Araujo, S. Chakraborty, P. Shanbogh, N. Sundaram, R. Ahuja and P. Barpanda, *J. Mater. Chem. A*, 2015, 3, 18564-18571
- [32] G. Kresse and J. Furthmuller, *Phys. Rev. B: Condens. Matter Mater. Phys.*, 1993, 47, 558.
- [33] G. Kresse and J. Hafner, *Phys. Rev. B: Condens. Matter Mater. Phys.*, 1996, 54, 11169.
- [34] J. P. Perdew, K. Burke and M. Ernzerhof, *Phys. Rev. Lett.*, 1996, 77, 3865.
- [35] S. L. Dudarev, G. A. Botton, S. Y. Savrasov, C. J. Humphreys and A. P. Sutton, *Phys. Rev. B*, 1998, 57, 1505.
- [36] T. Mueller, G. Hautier, A. Jain and G. Ceder, *Chem. Mater.*, 2011, 23 (17), 3854–3862.
- [37] C. G. Van de Walle and J. Neugebauer, *J. Appl. Phys.*, 2004, 95, 3851.
- [38] M. D. Radin and D. J. Siegel *Energy Environ. Sci.*, 2013, 6, 2370.
- [39] H. Jonsson, G. Mills and K. W. Jacobsen, in *Classical and Quantum Dynamics in Condensed Phased Simulations*, ed. B. J. Berne, G. Ciccotti and D. F. Coker, World Scientific, River Edge, NJ, 1998, p. 385.
- [40] G. Henkelman and H. J. Jonsson, *Chem. Phys.*, 2000, 113, 9978.
- [41] K. Momma and F. Izumi, *J. Appl. Crystallogr.*, 2011, 44, 1272-1276.
- [42] A. Van der Ven, C. Marianetti, D. Morgan and G. Ceder, *Solid State Ionics*, 2000, 135, 21–32.
- [43] C. Frayret, A. Villesuzanne, N. Spaldin, E. Bousquet, J. Chotard, N. Recham and J. Tarascon, *Phys. Chem. Chem. Phys.*, 2010, 12, 15512-15522.
- [44] S. C. Chung, P. Barpanda, S. I. Nishimura, Y. Yamada and A. Yamada, *Phys. Chem. Chem. Phys.*, 2012, 14, 8678.
- [45] F. Zhou, M. Cococcioni, C. A. Marianetti, D. Morgan and G. Ceder, *Phys. Rev. B*, 2014, 70, 235121.
- [46] M. S. Islam and C. A. J. Fisher, *Chem. Soc. Rev.*, 2014, 43, 185.
- [47] G. K. P. Dathar, D. Sheppard, K. J. Stevenson and G. Henkelman *Chem. Mater.*, 2011, 23 (17), 4032–4037.

- [48] K. Hoang and M. Johannes, *Chem. Mater.*, 2011, 23 (11), 3003–3013.
- [49] J. M. Clark, C. Eames, M. Reynaud, G. Rousse, J. Chotard, J. Tarascon and M. S. Islam *J. Mater. Chem. A*, 2014, 2, 7446-7453.
- [50] L. L. Wong, H. M. Chen and S. Adams, *Phys. Chem. Chem. Phys.*, 2015, 17, 9186.
- [51] P. M. Panchmatia, A. R. Armstrong, P. G. Bruce and M. S. Islam, *Phys Chem Chem Phys.*, 2014, 16(39), 21114-8.
- [52] K. Kang, D. Morgan and G. Ceder, *Phys. Rev. B*, 2009, 79, 014305.